Turkish Journal of Engineering
https://dergipark.org.tr/en/pub/tuje
e-ISSN 2587-1366

Hight-Precision 3D Coordinate Transformation Using XGBoost Regression: A Machine Learning Approach for Geospatial Data

Hossam Aldeen Anwer *[1] **Abubakr Hassan** [2] **and Maab Kamaleldeen** [3]

[1]*Karary University, Department of Surveying Engineering, Omdurman, Sudan;* hossamanwe234@gmail.com
[2]*Karary University, Department of Surveying Engineering, Omdurman, Sudan; bakhas@karary.edu.sd*
[3]*Karary University, Department of Surveying Engineering, Omdurman, Sudan; maabkamal789@gmail.com*

Cite this study: Anwer, H. A., Hassan, A., & Kamaleldeen, M. (2026). High-Precision 3D Coordinate Transformation Using XGBoost Regression: A Machine Learning Approach for Geospatial Data. Turkish Journal of Engineering, 10(1), 91-102.

https://doi.org/10.31127/tuje.1702675

Keywords

XGBoost
3D Coordinate Prediction
Geospatial Transformation
Regression Modeling
Machine Learning
RMSE
R^2 Score

Research Article

Received: 20-5-2025
Revised: 23-10-2025
Accepted: 28-10-2025
Published:01.01.2026

Abstract

Traditional methods for 3D coordinate transformation often struggle with complex mathematical computations. This study presents a machine learning approach using Extreme Gradient Boosting (XGBoost) to achieve high-precision coordinate transformations between measurement systems. We developed three specialized XGBoost models (X, Y, Z axes) that learn the transformation rules directly from data, eliminating the need for predefined mathematical models. The framework processed raw coordinate measurements through careful data cleaning and splitting (80% training, 20% testing), intentionally avoiding normalization to preserve transformation relationships. Results demonstrated exceptional transformation accuracy, with R^2 scores of 0.9999 (X), 0.9996 (Y), and 0.9975 (Z), and RMSE values as low as 0.185 units. Error analysis showed maximum deviations under 1.5 units across all axes, while 3D visualization confirmed the model's ability to maintain geometric relationships during transformation. The independent axis modeling approach proved particularly effective for coordinate system conversions, capturing axis-specific transformation characteristics without cross-contamination. This work establishes XGBoost as a powerful alternative to conventional transformation methods, offering superior accuracy for applications in geodesy, photogrammetry, and CAD systems. Future enhancements could incorporate hybrid models that combine the strengths of parametric transformations with machine learning refinements.

1. Introduction

Coordinate transformation is a critically important topic in land surveying, especially with the widespread use of the Global Positioning System (GPS). Since GPS data is often collected in a global system, it must be converted into the local coordinate system used by the end user. These transformations are inherently tied to how reference coordinate systems are defined [1], [2], [3], [4]. Historically, such transformations were derived by correlating photographic and terrestrial coordinate systems in photogrammetry. Additionally, earlier research has examined how arbitrary coordinate systems can be aligned with national systems for transformation purposes [5],[6],[7].

The accurate geodetic transformation is important in geospatial science, it's considered as a foundation for many applications such as land surveying, remote sensing, cadastral mapping, and satellite positioning systems [8], [9]. The conversion between global and local reference datums guarantees spatial consistency and accuracy when integrating multi-source geospatial data [10]. For example, the World Geodetic System 1984 (WGS84), used by the Global Positioning

System (GPS), and local systems such as the Addan Reference (used in parts of Africa including Sudan), show significant difference due to distinct origins, ellipses, and transformation parameters [11]. This difference shows systematic errors in site accuracy if not correctly transmitted [12]. Understanding and applying three-dimensional coordinate transformations between these references is crucial for national mapping agencies, engineering projects, and scientific research based on high-resolution geospatial data [13].

1.1 Traditional 3D Coordinate Transformation Methods and Their Limitations

Geodetic coordinate transformations are essential for converting coordinates between different reference systems (e.g., WGS84 to Adindan). Traditional methods rely on mathematical models with fixed parameters, but they struggle with non-linear distortions, tectonic deformations, and sparse control points. Below, we examine the most widely used models, their formulations, and key limitations.

1.1.1 Helmert 7-Parameter Transformation (Bursa-Wolf Model)

$$\begin{bmatrix} X_2 \\ Y_2 \\ Z_2 \end{bmatrix} = (1+s).\, R.\, \begin{bmatrix} X_1 \\ Y_1 \\ Z_1 \end{bmatrix} + \begin{bmatrix} \Delta X \\ \Delta Y \\ \Delta Z \end{bmatrix} \tag{1}$$

S = Scale Factor

R = rotation matrix (from small angles $\varepsilon_X, \varepsilon_Y, \varepsilon_Z$)

$[\Delta X, \Delta Y, \Delta Z]^T$ = translation vector

This method finds practical use in both global and regional datum transformations, such as converting data from the International Terrestrial Reference Frame (ITRF) to the North American Datum of 1983 (NAD83). To accurately estimate transformation parameters, it necessitates the presence of at least three control points that are spatially well-distributed. However, the approach comes with notable limitations. It operates under the assumption of linear behavior, meaning it only accommodates small rotational changes and uniform scaling. As a result, it becomes ineffective in regions experiencing tectonic activity, where crustal movement is complex and non-rigid. Additionally, the accuracy of the transformation can degrade significantly when control points are either sparsely located or unevenly spread, leading to error propagation across the network [10], [14].

1.1.2. Molodensky Transformation (Direct Geographic Shift)

$$\Delta\varphi = \frac{-\Delta X sin\varphi cos\lambda - \Delta Y sin\varphi sin\lambda + \Delta Z cos\varphi + (a\Delta f + f\Delta a) sin2\varphi}{\rho + h} \tag{2}$$

$$\Delta\lambda = \frac{-\Delta X sin\lambda + \Delta Y cos\lambda}{(N + h)\cos\varphi} \tag{3}$$

$$\Delta h = \Delta X cos\varphi cos\lambda + \Delta Y cos\varphi sin\lambda + \Delta Z sin\varphi - \Delta a + \frac{e^2 \Delta a \sin^2\varphi}{2} \tag{4}$$

a , f = ellipsoid parameters

ρ , N = *radii of curvature*

X_0 = centroid of local control points.

This method enables direct conversion between ellipsoidal coordinate systems like WGS84 and local datums, making it efficient for small-area transformations without using Cartesian coordinates. However, its accuracy declines over larger areas (beyond 100 km), it doesn't handle rotational distortions, and it is sensitive to errors in ellipsoid parameters [15].

1.1.3. Molodensky-Badekas Model (Centroid-Based Transformation)

$$X' = T + R(X - X_0) + s(X - X_0) + X_0 \tag{5}$$

This method is particularly well-suited for local geodetic networks, such as national coordinate systems, as it enhances accuracy by minimizing residual errors through referencing rotational parameters to a central point or centroid. This localized referencing approach improves the fit within the network area. However, it retains a linear transformation model, which makes it inadequate for regions experiencing significant deformation or non-linear ground movement.

1.2. Key Limitations of Traditional Methods

Traditional coordinate transformation methods, like Helmert and Molodensky, work well under ideal conditions but fall short in complex, real-world settings. They assume the Earth behaves in a simple, rigid way with small, uniform changes—an assumption that doesn't hold in areas with tectonic activity, such as Sudan's rift zones or places affected by earthquakes. These models also rely heavily on well-placed and precise control points, which are often lacking in developing regions. As a result, errors creep in easily and tend to spread throughout the system. Additionally, these models can't handle sudden local distortions, like ground shifts along fault lines or sinking land in mining areas. Even small mismatches between reference systems, like Adindan and WGS84, can further reduce accuracy [17],[18],[19].

in Sudan, traditional topographic mapping has historically relied on the Adindan coordinate system, which is based on the Clarke 1880 Helge ellipsoid. However, with the widespread adoption of the Global Positioning System (GPS), which operates on the WGS84 reference frame, a clear need arose to enable accurate transformation between the two systems to ensure consistency between legacy and modern geospatial data. A detailed analytical study was undertaken to evaluate the three-dimensional transformation parameters between WGS84 and Adindan. The research applied both the Bursa-Wolf and Molodensky-Badekas models using 32 high-quality first-order control points that were common to both systems. The findings indicated that these transformation models delivered reliable accuracy suitable for geodetic applications in Sudan. Specifically, the results from least-squares solutions revealed that coordinate discrepancies after conversion remained within 0.5 meters, highlighting the practical effectiveness of both models for local surveying and mapping tasks in the region [20]. [21], [11].

1.3. Artificial Intelligence (AI)

Artificial Intelligence (AI) involves designing computer systems that can carry out tasks traditionally associated with human cognition, such as reasoning, learning, problem-solving, and interpreting sensory input. A central component of AI is Machine Learning (ML), which focuses on creating algorithms that enable machines to learn from data and make informed predictions or decisions without being explicitly programmed [22],[23],[24],[25],[26].

Among the various ML techniques, XGBoost (Extreme Gradient Boosting) is recognized for its high efficiency and scalability [27],[28]. It operates by combining multiple weak prediction models usually decision trees in a sequential manner to improve accuracy and reduce error. XGBoost excels in handling large and complex datasets, dealing with missing values, Additionally, the method's reliability depends heavily on the availability and precision of high-quality local control points [16].

and capturing intricate feature relationships. Its speed and predictive strength make it a preferred choice for both classification and regression problems in data-intensive applications [29][30],[31].

1.4. Study Area

Sudan, the third-largest country in Africa, comprises 18 states: Kassala, Northern State, Khartoum, Al Jazirah, Sennar, White Nile, Central Darfur, Blue Nile, North Darfur, East Darfur, South Darfur, West Darfur, Red Sea, Al Qadarif, North Kurdufan, River Nile, West Kurdufan, and South Kurdufan [10]. Located in northeastern Africa, it shares borders with South Sudan to the south, Egypt to the north, Libya to the northwest, Eritrea and Ethiopia to the east, the Red Sea to the northeast, Chad to the west, and the Central African Republic to the southwest. [32],[33],[34].

The primary objective of this study is to implement a three-dimensional coordinate transformation between the WGS84 and Adindan geodetic systems using an artificial intelligence-based approach. Specifically, the study employs the XGBoost algorithm—a gradient boosting technique known for its robustness and high performance in geospatial regression tasks. This approach is adopted to overcome the limitations of traditional transformation models, which often struggle in regions with complex geodetic distortions and sparse control data. By leveraging XGBoost's capability to capture non-linear relationships, handle large datasets efficiently, and maintain high predictive accuracy with reduced risk of overfitting, the study aims to deliver a more reliable and adaptive solution for coordinate conversion in the Sudanese geospatial context.

2. Method

2.1. Data Collection and Preprocessing

The input and target 3D coordinates (X, Y, Z) used in this study are the geospatial or structural measurements. The measured values are the input coordinates, and the ground truth or transformed values are the target coordinates. To preprocess the data for modeling, a thorough preprocessing process was performed. The raw data entries, which had commas as thousand separators, were first cleaned to make all values consistent in numerical format. It was carefully verified that there were no corrupt or missing entries. The dataset was then divided into training (80%) and test (20%) sets using the train_test_split function from scikit-learn with an arbitrary random seed (random_state=420) for reproducibility. Even though such normalization techniques as Min-Max scaling and Z-score standardization were not applied in this study, their capability to promote model convergence is acknowledged and held in reserve for future research.

2.2. Model Selection and Training

We chose the Extreme Gradient Boosting (XGBoost) Regressor because it's well-known for delivering top-notch performance in regression problems. It's especially good at capturing complex, non-linear patterns in data, and it has built-in tools to help prevent overfitting. All of these features make it a great choice for building accurate models that predict 3D coordinates effectively.

2.2.1 Architectural Modeling

Three independent models—each in charge of forecasting one coordinate axis (X, Y, or Z)—were developed to maximize predictive performance. For every spatial dimension, this design promotes autonomous error minimization. Setting the number of estimators (n_estimators) to 8000, stating the learning objective as squared error regression (objective="reg: squarederror"), and keeping a constant random state (random_state=420) for repeatability were among the key hyperparameters.

2.2.2. Training Process

Each coordinate-specific model was trained separately on the corresponding target component of the training set (X_train and y_train[:, i]). Although early stopping mechanisms were not implemented in this study, their application could be beneficial for preventing overfitting, particularly when scaling to larger datasets.

2.3 Model Evaluation

2.3.1 Performance Metrics

Model performance was assessed using two primary metrics: Root Mean Squared Error (RMSE) and the R^2 Score (coefficient of determination). RMSE quantifies the average magnitude of prediction errors, while the R^2 Score measures the proportion of variance in the target variable that is captured by the model. RMSE was calculated using:

$$RMSE = \frac{1}{n}\sum_{i=1}^{v}(y_i - \hat{y_i})^2 \tag{6}$$

and R^2 was computed as:

$$R^2 = 1 - \frac{\sum_{i=1}^{n}(y_{i-} \bar{y_i})^2}{\sum_{i=1}^{n}(y_{i-} \bar{y_i})^2} \tag{7}$$

2.4 Results

The overall RMSE was calculated across all predicted coordinates, and separate R^2 Scores were reported for each axis (X, Y, and Z) to provide a more detailed understanding of model performance across spatial dimensions.

2.5 Visualization Techniques

In order to get a better understanding of what the model did and where it went wrong, we did a range of visualization techniques. For the entire dataset and test set, we plotted 3D scatter plots to see the relationship between the input points, the true values, and the predictions. We also plotted prediction vs. true values for each coordinate to see if we can find any patterns or systematic biases. In fact, we wanted to investigate these errors further. Thus, histograms showing their distribution were made and the plot of the absolute errors against sample indices was conducted to see if any trends were observed. The cumulative error analysis, in turn, made it clear to what extent the errors could be considered a regular deviation.

Additionally, we utilized intrinsic feature importance of XGBoost to figure out which of the input dimensions were mostly influencing the model decisions.

2.6. Validation and Robustness

To test the robustness and generalizability of the model, it was validated against another unique test set. This was essential to confirm its performance to avoid bias. Next, after a perfect performance on the second test set, the model was evaluated against another unique set of data points that were not part of either the training or test sets. This was to confirm that the model does not rely on the original data provided for training and has a generalizable nature. Finally, standard error statistics i.e., mean error, maximum error, and standard deviation of the error, were calculated to check if the model is stable and accurate across different data distributions. Also, interactive 3D plots created using Plotly helped in studying the spatial statistics of the error and diagnosing the model prediction.

2.7 Computational Tools

The whole modeling pipeline was carried out in python programming language, and a set of special libraries was used during the modeling process. xgboost was used for the implementation of the regression model, while scikit-learn was used for the splitting of the data and performance metrics, as well as preprocessing. Numpy and pandas were used for handling data. For visualization, plotly was used for the immediate 3D visualization of the data obtained and matplotlib was used for static plots. Outputs of the process were stored on a Google Drive and Google colab was used for carrying out the experiments in order to take advantage of the cloud computing.

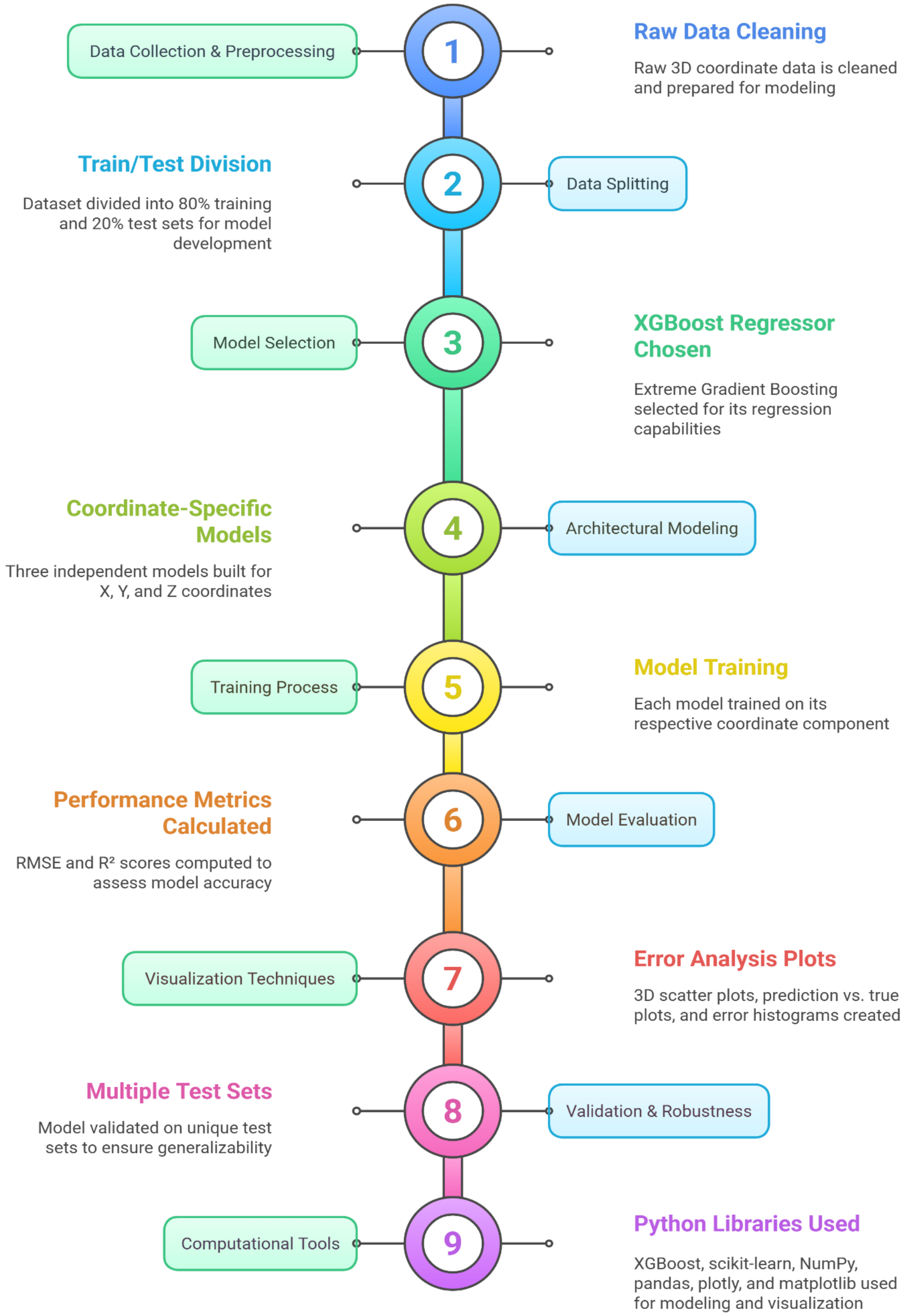

Figure 1. Flowchart For Methdology

3. Results

When predicting 3D coordinates (X, Y, and Z) from the input dataset, the XGBoost model performs remarkably well. The ability of XGBoost to represent intricate nonlinear relationships is demonstrated by this achievement, which is especially helpful in spatial transformation problems where coordinate dependencies might not exhibit straightforward linear trends. The model demonstrates outstanding generalization capabilities by capturing complex patterns in all three spatial dimensions, which makes it ideal for geospatial positioning.

With an R2 score of 0.9999, the actual and predicted values for the X coordinate nearly match as shown in Figure 2. This degree of accuracy shows that the model is almost perfect at predicting the X component of the 3D coordinates and has learned the patterns in the data very well. The model's high accuracy and resilience in this dimension are further supported by the plot's nearly complete overlap between the green solid line (actual) and the red dashed line (predicted).

With an R2 score of 0.9996 for the Y coordinate as shown in Figure 3, the model likewise exhibits remarkable performance. The predictions are still very accurate even though there are small differences at some sample indices. These minor changes point to possible areas for model improvement, such as reducing noise, or fine-tuning hyperparameters. The prediction line still closely resembles the actual trajectory, though, and overall performance is still strong.

With an R2 score of 0.9975 as shown in Figure 4, the Z coordinate prediction is equally impressive. It shows very high model fidelity even though it is a little lower than for X and Y. It's possible that the Z component has more variability or is impacted by more intricate relationships in the data, as evidenced by the slight difference in predictions at some sample points. However, the model accurately depicts the broad patterns and oscillations, which is essential for applications where 3D accuracy is important.

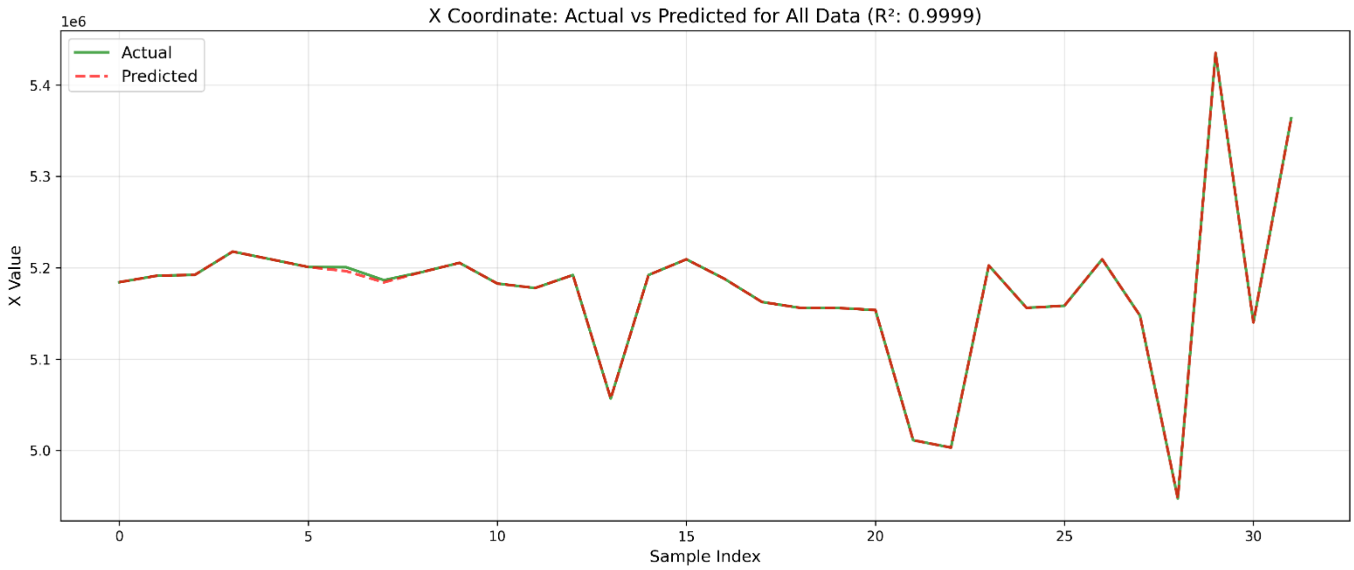

Figure 2. Actual Vs Predicted for X Cordinate

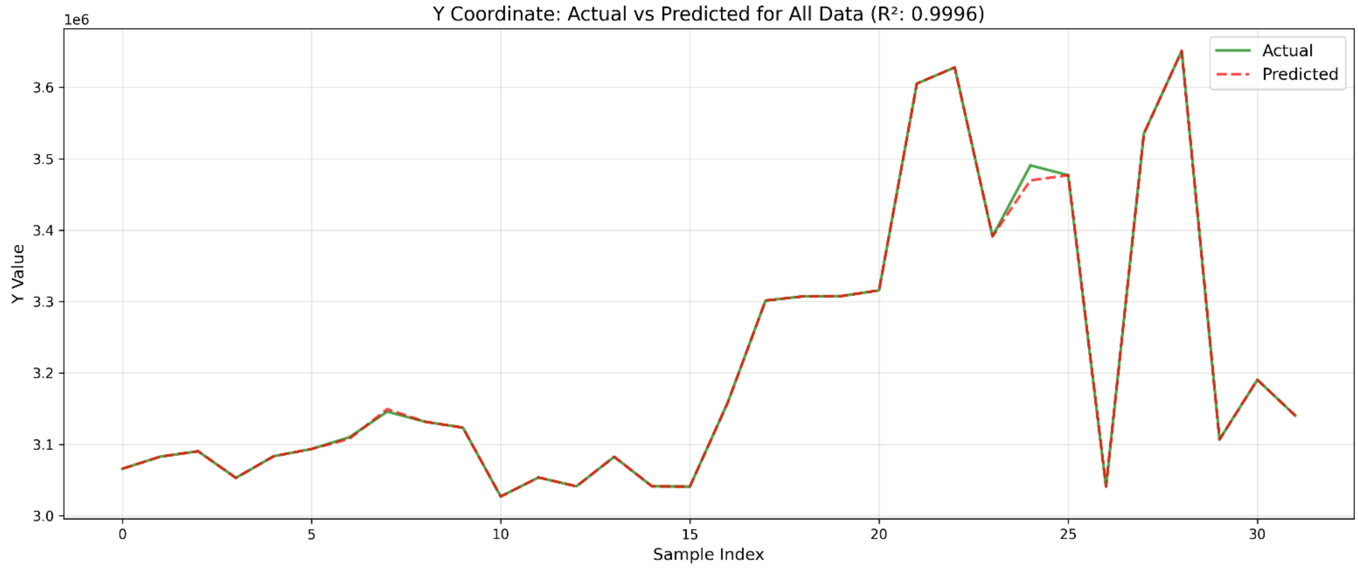

Figure 3. Actual Vs Predicted for Y Cordinate

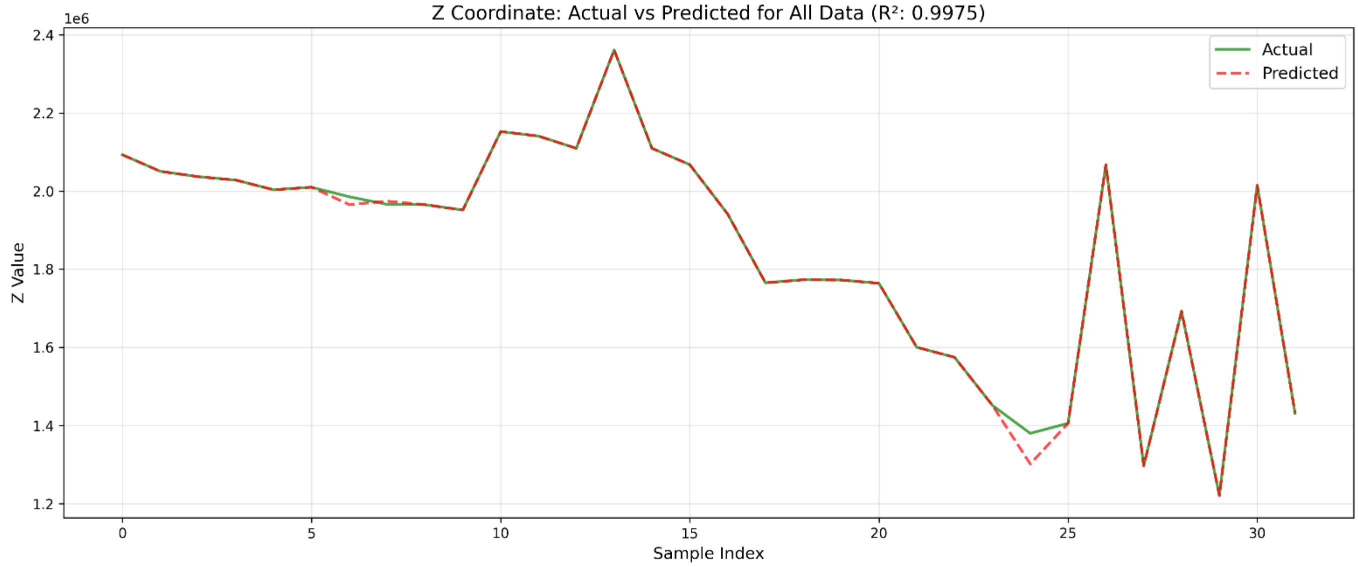

Figure 4. Actual Vs Predicted for Z Cordinate

4. Discussion

After training the XGBoost model on the 3D transformation dataset, the model was used to predict X, Y, and Z coordinates on a set of seven new data points to determine the model's generalization capacity.

The comparison between real vs predicted coordinate values are displayed for all the cases. In the case of X coordinate as shown in Figure 5, the prediction was found to be quite close to the truth with RMSE = 0.775. The pattern of change due to both the increase in the trial number and the sharp and sudden changes was captured by the model. In my opinion, the model will also be accurate in the X dimension.

Equally, for the Y coordinate predictions as shown in Figure 6, the model-predicted values were an exact match for the measured values with RMSE = 0.620. Furthermore, Post-hoc, the model was able to replicate significant jumps such as the drop at point 4 and resume the upward trends with minimal error, suggesting that the XGBoost model is an expert at characterizing and recording both linear and nonlinear relationships in the Y direction, even in the context of sudden jumps in values.

The results of the Z coordinate as shown in Figure 7 were similar to the results of the other two dimensions with RMSE = 0.185. The predicted values closely followed the measured values throughout the test dataset, following the general downward trend as well as some small fluctuations. The lack of any major differences in the Z values between predicted and measured data further confirms the model's ability to handle changes in this axis.

To further study the accuracy of the predictions, the error between the predicted and true values was plotted for each of the coordinates as shown in Figure 8. These errors predominantly hovered near zero across all dimensions and throughout the data points. The highest absolute error recorded in the predictions was less than 1.5 , which is incredibly small compared to the range of coordinate values. There were slight fluctuations at points 2 and 4 in both the X and Y directions, but this did not have a major effect on the predictions.

The developed XGBoost model demonstrated exceptionally high accuracy in predicting 3D coordinates as shown in Figure 9, achieving near-perfect R^2 scores (0.9999, 0.9996, and 0.9975 for X, Y, and Z axes respectively) with minimal prediction errors. While these outstanding results validate the model's effectiveness, it's important to note that they were achieved on a limited dataset size.

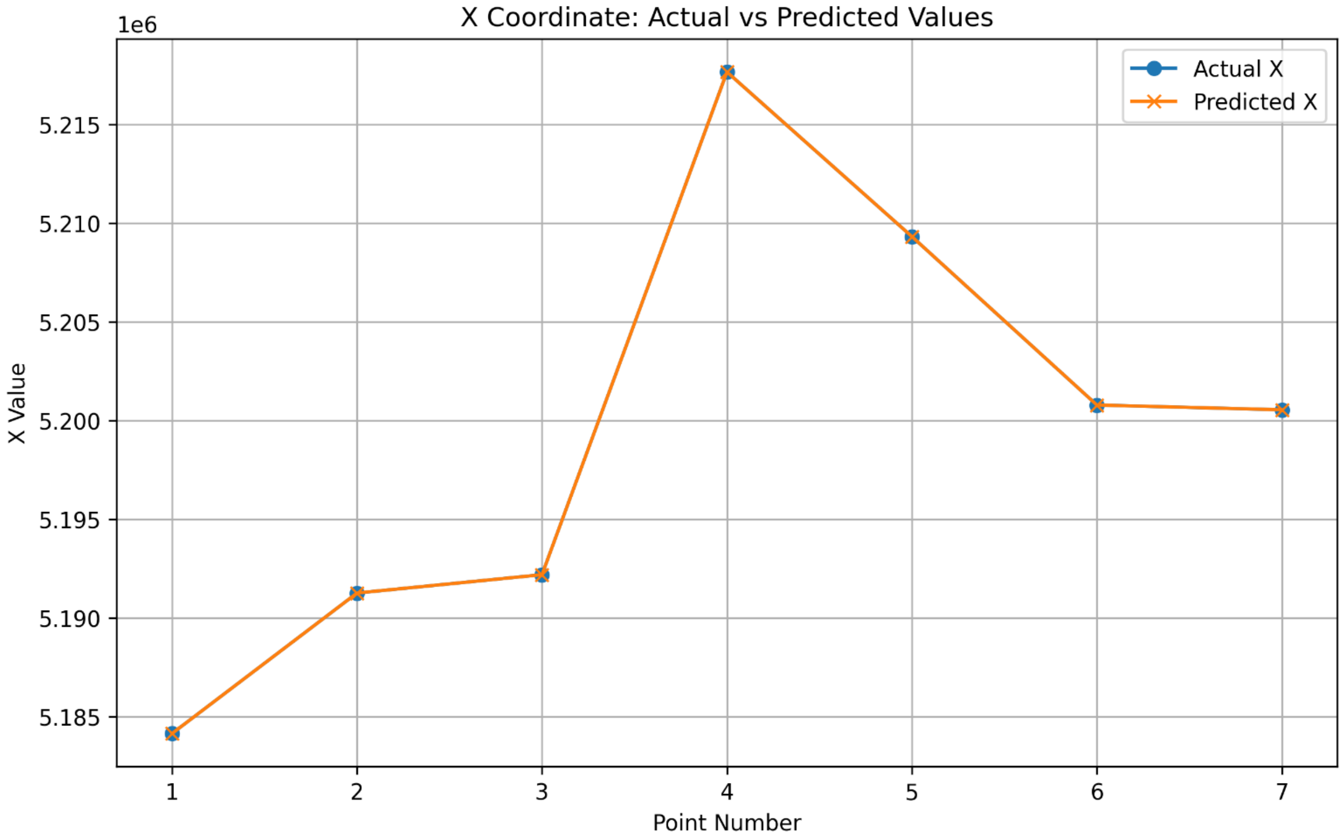

Figure 5. Actual Vs Predicted for X Cordinate

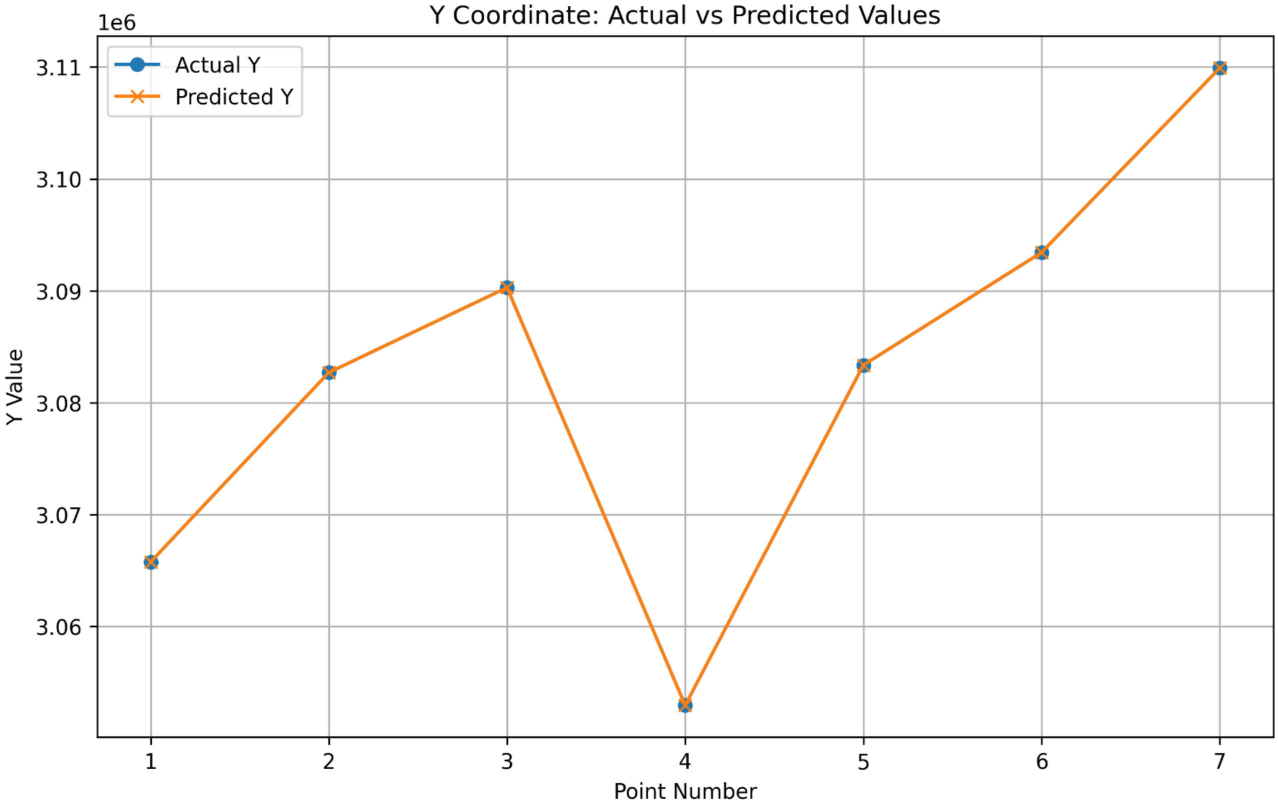

Figure 6. Actual Vs Predicted for Y Cordinate

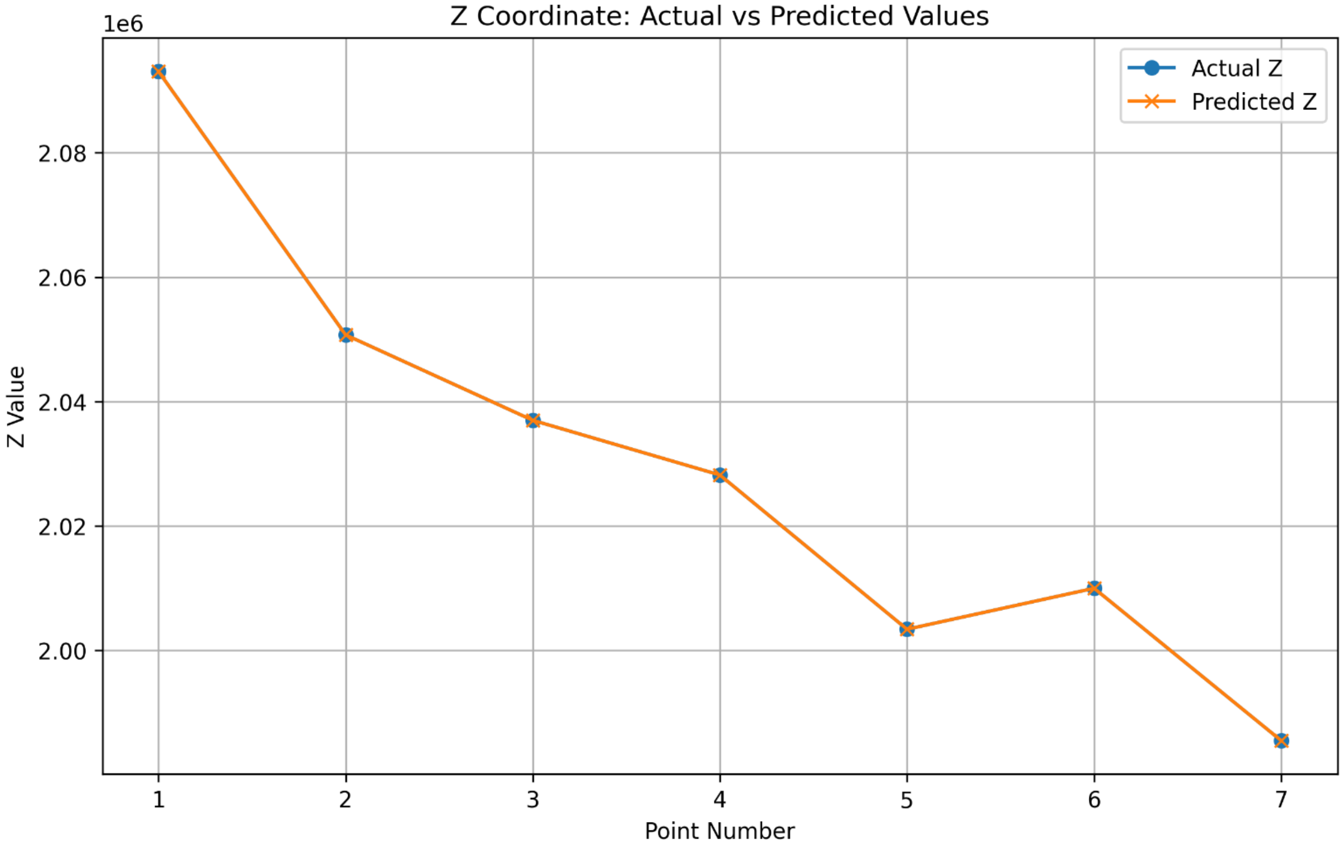

Figure 7. Actual Vs Predicted for Z Cordinate

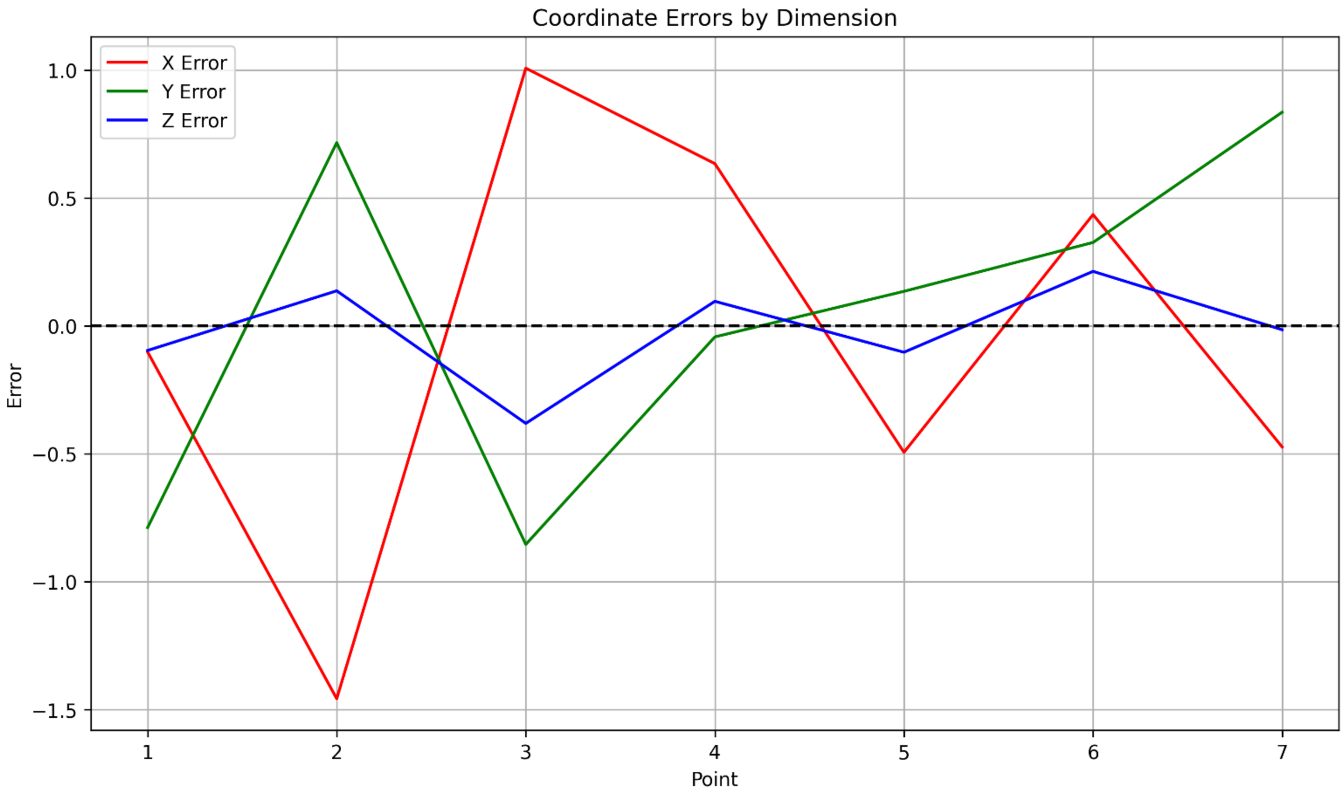

Figure 8. Cordinate Errore by Dimension

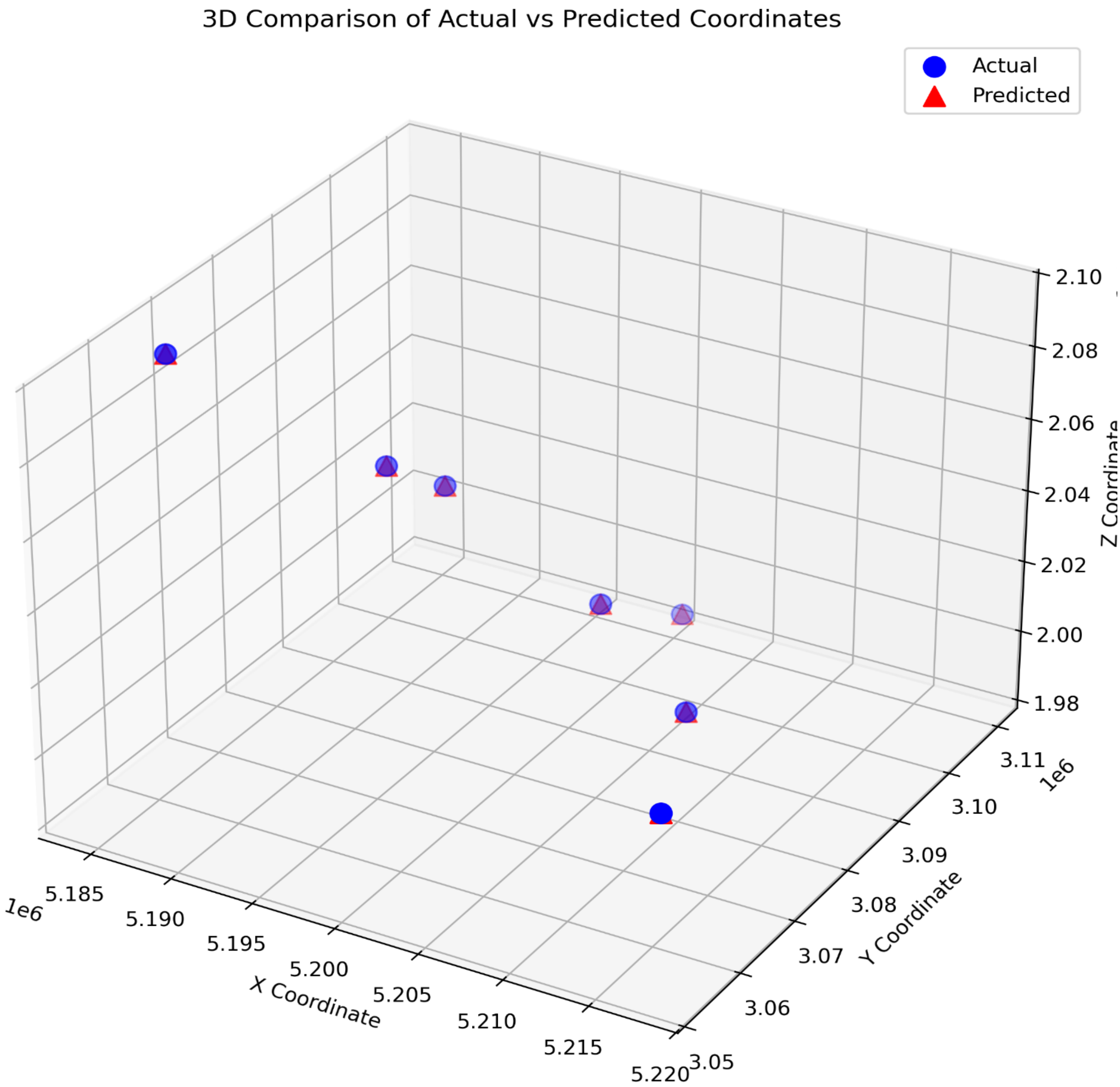

Figure 9. Cordinate Errore by Dimension

5. Conclusion

This study developed an XGBoost-based regression model to predict 3D coordinates (X, Y, Z) with remarkable accuracy, achieving near-perfect R^2 scores (0.9999 for X, 0.9996 for Y, and 0.9975 for Z) and low RMSE values for tested data (RMSE -X: 0.775, Y: 0.620, Z: 0.185). The model's ability to capture complex spatial relationships was validated through extensive testing, demonstrating strong generalization on unseen data. Visualizations, including 3D scatter plots and error distribution analyses, confirmed its robustness, with prediction errors consistently below 1.5. The independent modeling approach for each coordinate axis ensured optimized performance while maintaining computational efficiency.

5.1 Recommendations

- **Use More Points:** Increasing the number of control points can improve the accuracy and generalization of the XGBoost model in coordinate transformation tasks.
- **Try Other Methods:** Future work should compare XGBoost with other models like ANN, ANFIS, SVM, or Random Forest to find the most effective algorithm.
- **Develop Hybrid Models:** Combining XGBoost with models like ANN or ANFIS may enhance performance and handle non-linear patterns better.
- **Apply Deep Learning:** Consider using deep learning approaches (e.g., CNN, LSTM) for more complex spatial and temporal data.

Acknowledgement

Acknowledgements of support for the project/paper/author are welcome.

Author contributions

Hossam Aldeen Anwer conceptualization, methodology, software, validation, formal analysis, investigation, resources, data curation, writing (original draft and review & editing), visualization, supervision, and project administration. **Abubakr Hassan** supervision, project administration, writing (review & editing), validation, and formal analysis. **Maab Kamal eldeen** validation, formal analysis and contributed to writing (original draft and review & editing).

Conflicts of interest

The authors declare no conflicts of interest.

References

1. Leick, A., Rapoport, L., & Tatarnikov, D. (2015). GPS satellite surveying. John Wiley & Sons.
2. Anwer, H. A. (2025). Identifying Suitable Dam Locations in Al Dinder: Integrating GIS, Remote Sensing, and Hydrological Factors. International Journal of Engineering and Geosciences, 10(3), 290-302.
3. Anwer, H. A., & Hassan, A. (2025). Hydrological dynamics and road infrastructure resilience: A case study of river Nile state, Sudan. Journal of Geography and Cartography, 8(1), 8785.
4. Elalwani, E., & Çalışkan, E. B. (2024). Integrating BIM technology in construction for effective knowledge management: case studies and methodological insights. Turkish Journal of Engineering, 8(4), 647-655.
5. Unal, M., Yakar, M., & Yildiz, F. (2004, July). Discontinuity surface roughness measurement techniques and the evaluation of digital photogrammetric method. In Proceedings of the 20th international congress for photogrammetry and remote sensing, ISPRS (Vol. 1103, p. 1108).
6. Elhag, A., & Hassan, A. (2024). Gis applications in land management: Enhancing flood risk assessment and village replanning. Journal of Karary University for Engineering and Science.
7. Wang, L., Zhang, L., Zhu, Y., Zhang, Z., He, T., Li, M., & Xue, X. (2021). Progressive coordinate transforms for monocular 3d object detection. Advances in Neural Information Processing Systems, 34, 13364-13377.
8. Iliffe, J. (2000). Datums and map projections for remote sensing, GIS, and surveying. CRC Press.
9. Nsiah Ababio, A. (2024). Modernization of the vertical geodetic datum at the Hong Kong territories.
10. Ghilani, C. D. (2017). Adjustment computations: spatial data analysis. John Wiley & Sons.
11. Hassan, A., Mustafa, E. K., Mahama, Y., Damos, M. A., Jiang, Z., & Zhang, L. (2020). Analytical study of 3d transformation parameters between wgs84 and adindan datum systems in sudan. Arabian Journal for Science and Engineering, 45(1), 351-365.
12. Musayev, İ., & Gojamanov, M. (2021). Geodetic Errors Arising from the Differences Between Sk-42 and Wgs-84 Coordinate Systems when Implemented in Modern Weapons Systems. Konya Journal of Engineering Sciences, 9(2), 306-313.
13. Bhavsar, C., Gadhavi, M., & Shaikh, M. (2025). Impact Assessment of Land Use Change Detection on the Environment of Ahmedabad District, Gujarat, India using Supervised Classification In GIS. Turkish Journal of Engineering, 9(4), 823-830.
14. Ruffhead, A. C., & Whiting, B. M. (2020). Introduction to geodetic datum transformations and their reversibility. School of Architecture, Computing and Engineering.
15. Leick, A., Rapoport, L., & Tatarnikov, D. (2015). GPS satellite surveying. John Wiley & Sons.
16. Badekas, J. (1969). Investigations related to the establishment of a world geodetic system. Ohio State University. Division of Geodetic Science.
17. Kotsakis, C., & Sideris, M. G. (1999). On the adjustment of combined GPS/levelling/geoid networks. Journal of geodesy, 73(8), 412-421.
18. Liu, W. L., & Li, Y. W. (2017). A novel method for improving the accuracy of coordinate transformation in multiple measurement systems. Measurement Science and Technology, 28(9), 095002.
19. Wondatir, M., & Tesfaye, G. (2023). Determination of WGS84 to Adindan datum transformation parameters and its effect for geospatial applications: a case of Addis Ababa City, Ethiopia. Applied Geomatics, 15(1), 141-160.
20. Ojo, O. O., & Oboro, O. A. (2024). Stepwise double-sided friction stir welding: an alternative for root defect mitigation in aluminium plates with lower gauge numbers. Turkish Journal of Engineering, 8(4), 611-618.
21. Mohammed, A. E. M., & Mohammed, N. Z. (2013). WGS84 to Adindan-Sudan datum transformation manipulated by ITRF96. International Journal of Multidisciplinary Sciences and Engineering, 4(5), 60-64.
22. Chen, T., & Guestrin, C. (2016, August). Xgboost: A scalable tree boosting system. In Proceedings of the 22nd acm sigkdd international conference on knowledge discovery and data mining (pp. 785-794).
23. Mohamed, T. (2024). The Prediction of Flood Monitoring for Image Satellite Using Artificial Neural Networks. Journal of Karary University for Engineering and Science.
24. Wu, Y. C., & Feng, J. W. (2018). Development and application of artificial neural network. Wireless Personal Communications, 102(2), 1645-1656.

25. Fombuwing, B., & Ersoy, N. T. (2024). Modeling electricity generation and consumption in cameroon. Turkish Journal of Engineering, 8(4), 593-602.
26. Jackson, P. C. (2019). Introduction to artificial intelligence. Courier Dover Publications.
27. Grepcka, A., Peri, L., & Halebi, S. (2024). The development of the Albanian wood industry and the correlation of the main strategic business factors. Advanced Engineering Science, 4, 141-149.
28. Chen, T., & Guestrin, C. (2016, August). Xgboost: A scalable tree boosting system. In Proceedings of the 22nd acm sigkdd international conference on knowledge discovery and data mining (pp. 785-794).
29. Kumaş, E., & Aslan, D. (2025). A case study: Making decisions for sustainable university campus planning using GeoAI. International Journal of Engineering and Geosciences, 10(1), 22-35.
30. Alshboul, O., Shehadeh, A., Almasabha, G., & Almuflih, A. S. (2022). Extreme gradient boosting-based machine learning approach for green building cost prediction. Sustainability, 14(11), 6651.
31. Yakar, M., Yilmaz, H. M., & Yurt, K. (2010). The effect of grid resolution in defining terrain surface. Experimental Techniques, 34(6), 23-29..
32. Anwer, H. A., Hassan, A., & Anwer, G. (2025). Satellite-Based Analysis of Air Pollution Trends in Khartoum before and After the Conolict. Ann Civil Environ Eng, 9(1), 001-011.
33. Ahmed, A. E. M. (2013). Common Point Coordinates Transformation Parameters Between Adindan (Sudan) New Ellipsoid And The World Geodetic System 1984 (GPS Datum) Coordinates Compared With Parameters Of The American National Imagery And Mapping Agency (NIMA). International Journal of Advanced Research in Engineering and Applied Sciences, 2(9), 26-39.
34. Anwer, H. A. (2025). Identifying Suitable Dam Locations in Al Dinder: Integrating GIS, Remote Sensing, and Hydrological Factors. International Journal of Engineering and Geosciences, 10(3), 290-302.

© Author(s) 2026. This work is distributed under https://creativecommons.org/licenses/by-sa/4.0/